




Co-encapsulation of curcumin and salicylic acid in mucoadhesive polymer nanoparticles

Cristian Moreno¹, Jorge Forero¹, Yolima Baena¹, Leon Perez^{2*} 

¹Departamento de Farmacia, Facultad de Ciencias, Universidad Nacional de Colombia, Bogotá, Colombia.

²Departamento de Química, Facultad de Ciencias, Universidad Nacional de Colombia, Bogotá, Colombia.

ARTICLE HISTORY

Received on: 14/07/2023

Accepted on: 27/11/2023

Available Online: 04/01/2024

Key words:

Polymer nanoparticles, curcumin, salicylic acid, coencapsulation.

ABSTRACT

Colorectal cancer poses a significant global health challenge with high incidence and mortality rates, as reported by the World Health Organization. Natural compounds such as curcumin (Cur) and salicylic acid (SCA) have shown promising therapeutic effects against colorectal cancer. However, their oral administration is hindered by their low bioavailability. This study aimed to develop mucoadhesive nanoparticles capable of co-encapsulating Cur and SCA using a double-emulsion process. The copolymer m-PEG-b-PCL, which is considered a safe material for biomedical applications, was chosen as the polymeric precursor, while chitosan, which has mucoadhesive properties, served as the emulsion stabilizer. Through the optimization of drug concentrations, polymer molecular weights, and stabilizer type and concentration, a formulation composed of spherical nanoparticles with an average hydrodynamic diameter of 355 nm and an entrapment efficiency of 13.70% for Cur and 90.72% for SCA was obtained. The release kinetics showed sustained release over 24 hours. Moreover, these nanoparticles demonstrated strong adhesion to the colonic mucosa, presenting a potential localized drug delivery strategy. Co-encapsulation of Cur and SCA within mucoadhesive polymer nanoparticles holds great potential for significantly enhancing the therapeutic outcomes of colorectal cancer treatment.

INTRODUCTION

According to the World Health Organization, the global impact of colorectal cancer is significant, with nearly 935,000 deaths reported worldwide in 2020. It is a prevalent disease, ranking second in incidence and third in mortality [1]. In Latin America, the incidence of colorectal cancer is especially high among men, and mortality rates are rising in countries such as Uruguay, Chile, and Argentina [2].

Curcumin (Cur), a polyphenolic compound, has shown various therapeutic properties, including antiparasitic, antioxidant, anti-inflammatory, and pro-apoptotic effects in rectal cancer cells [3–5]. However, oral administration can be limited by its low solubility and rapid metabolism, leading to

low bioavailability and difficulty interacting with colonic cells [6,7]. Conversely, recent studies have indicated that salicylic acid (SCA) may reduce oxidative stress and prostaglandin production at the colonic level and modulate cytosolic glutathione peroxidase activity in the colon, potentially inhibiting cancer development in tissues [8,9]. Simultaneous administration of SCA and Cur may offer a synergistic effect in cancer treatment by simultaneously targeting multiple therapeutic targets.

The co-encapsulation of Cur and SCA in polymer nanoparticles is challenging because of their different chemical properties. Cur has been successfully encapsulated using various polymeric nanoparticles, liposomes, dendrimers, solid lipid nanoparticles, and nanostructured lipid carriers [10–13]. In contrast, SCA has been encapsulated in liposomal particles and inorganic structures such as silica and clay [14–16]. A promising alternative is to obtain polymer nanocapsules via double emulsification, which creates hydrophilic domains to host SCA and hydrophobic polymer matrices that can dissolve Cur, thereby enabling simultaneous encapsulation of both compounds.

*Corresponding Author

Leon Perez, Departamento de Química, Facultad de Ciencias, Universidad Nacional de Colombia, Bogotá, Colombia.

E-mail: ldperezp@unal.edu.co

This study aimed to determine the experimental conditions for obtaining mucoadhesive nanoparticles capable of co-encapsulating Cur and SCA using a double emulsion process. The selection of m-PEG-*b*-PCL as the polymeric precursor was based on its biodegradability, biocompatibility, and approval for use in biomedical applications by regulatory agencies such as the Food and Drug Administration [17,18]. Chitosan (CH), a cationic biopolymer, was used as an emulsion stabilizer to exploit its mucoadhesive properties against intestinal mucins [19,20]. This approach for the development of bicompartamental nanoparticles for simultaneous encapsulation and delivery of Cur and SCA with mucoadhesive properties has potential implications for enhancing therapeutic outcomes in the treatment of colorectal cancer. Mucoadhesion permits localized drug delivery, enabled by the high intestinal permeability of nanoparticles, which accumulate in specific intestinal sections. This strategy enhances drug bioavailability, reduces systemic toxicity, and increases patient compliance [21–23].

EXPERIMENTAL PART

Materials

Methoxy-poly(ethylene glycol) (mPEG) with a molecular weight of 2 kDa, ϵ -caprolactone (CL, 98%), tin octanoate [Sn(Oct)₂, 98%], Cur (Cur, $\geq 94\%$), low molecular weight CH, and polysorbate 80 were purchased from Sigma-Aldrich. Químicos el Alquimista provided SCA. All the other reagents and solvents were supplied by PanReac AppliChem. All procedures were performed using Type I water. Toluene was dried via reactive distillation with sodium using benzophenone as an indicator of humidity. Before use, mPEG was subjected to azeotropic distillation with dry toluene, and the CL was dried with calcium hydride to remove any residual moisture. The Murine colon was provided by Bioterium of the Department of Pharmacy at the National University. The tests reported in this study were approved by the ethics committee of the same institution through Act Number 15 of 7 April 2022 of the Faculty Council, Resolution 28 of 2022.

Synthesis of PEG-*b*-PCL

m-PEG-*b*-PCL copolymers were synthesized following previously reported procedures [10,24,25], with slight modifications to the method. For the synthesis of the PCL segment with a molecular weight of 40 kDa, mPEG (2 g, 1 mmol), CL (43 ml, 351 mmol), and Sn(Oct)₂ catalyst (162 μ l, 0.5 mmol) were combined in a round-bottom flask and 30 ml of toluene was added. The reaction mixture was stirred under an argon atmosphere at 110°C for 24 hours. After the completion of the reaction, the product was dissolved in dichloromethane (DCM) and precipitated with diethyl ether at 0°C. The resulting precipitate was filtered, washed, and dried under a vacuum for 24 hours at room temperature. ¹H-RMN (400 MHz, TMS) PEG δ (ppm) = 3.4 (s, CH₃-O-), 3.6 (s, -CH₂-CH₂-O-). PCL δ (ppm) = 1.4 (s, -C(O)-CH₂-CH₂-CH₂-), 1.6 (q, -CH₂-CH₂-CH₂-), 2.3 (t, -C(O)-CH₂-), 4.0 (t, -CH₂-O).

Co-encapsulation of Cur and SCA

The procedure employed in this study was adapted from a previous study [26]. In the first step, 0.3 ml of aqueous SCA (with concentrations ranging from 0 to 8 mg/ml, phase w_1)

was emulsified in 3 ml of an organic phase containing m-PEG-*b*-PCL with PCL segments of either 30 or 40 kDa (8 wt%), and Cur (with concentrations ranging from 0 to 3 mg/ml) dissolved in DCM (phase o). The emulsification process was performed using an Ultra Turrax T-10 (IKA, USA) equipped with a T-10N 8G shaft at 16,800 rpm for 15 minutes. The resulting initial emulsion (w_1/o) was then dropwise added to 12 ml of an aqueous phase (w_2) containing an external stabilizing agent, specifically polyvinyl alcohol (PVA) 0.5 wt% or low-molecular-weight CH 0.2 or 0.5 wt%. This mixture was homogenized at 19,000 rpm for 15 minutes, and the resulting double emulsion was magnetically stirred at 250 rpm for 2 hours at room temperature. After complete evaporation of DCM, the volume of the nanoparticle suspension was adjusted to 20.0 ml by adding water. Centrifugation at 5,000 rpm for 7 minutes was performed to separate the non-encapsulated Cur, and 50 μ l of the supernatant was withdrawn to measure the hydrodynamic diameter of the particles (D_h) and their ζ -potential. The remaining dispersion was concentrated by ultrafiltration in Amicon Ultra-4 10 kDa tubes and centrifuged at 7,000 rpm for 45 minutes. The filtrate was collected to determine the non-encapsulated SCA, and the concentrated suspension was resuspended in water to a final volume of 10.0 ml and frozen at -20°C. The drug-loaded nanoparticles were recovered by lyophilization for 72 hours and then subjected to further characterization.

Characterizations

Particle size and distribution measurement

Particle size and distribution analyses were performed by dynamic light scattering (DLS) using a Horiba SZ-100 instrument. Before the measurements, 50 μ l of each suspension was diluted in 5 ml type I water. The analyses were performed at 25°C using disposable cells.

Scanning electron microscopy (SEM)

SEM was performed using a Zeus instrument to analyze the morphology of the nanoparticles. Before analysis, 10 μ l of an aqueous dispersion of the sample was deposited onto a glass microscope coverslip, which was previously rinsed with NaOH. After drying, the sample was sputter-coated with a thin layer of gold to improve the conductivity and imaging quality. The SEM imaging was performed at an accelerating voltage of 20 kV.

Differential scanning calorimetry (DSC)

DSC was used to investigate the thermal properties of the empty nanoparticles and nanoparticles containing Cur and SCA, separately and simultaneously. The measurements were conducted using a Shimadzu DSC-60 Plus instrument. The samples were cooled from room temperature to -40°C and heated at a rate of 5°C/minute to 200°C.

Encapsulation efficiency (EE)

The %EE of SCA and Cur was determined by UV-vis spectrometry using a Shimadzu UV-1800 spectrophotometer. To determine the %EE of SCA, the non-encapsulated drug was measured by determining the concentration of SCA in the filtrate using Equation 1. For Cur, lyophilized formulations

were suspended in DCM, evaporated, dispersed in ethanol, and filtered before being subjected to UV-vis analysis at 426 nm. The %EE of Cur was calculated using Equation 2.

$$\%EE \text{ for SCA} = \frac{\text{amount of SCA in the feed} - \text{SCA in the supernatant}}{\text{amount of SCA in the feed}} \times 100 \quad (1)$$

$$\%EE \text{ for Cur} = \frac{\% \text{ Cur in the formulation}}{\% \text{ Cur in the feed}} \times 100 \quad (2)$$

The SCA and Cur were quantified by interpolation in a calibration plot. For the quantification of SCA, aqueous solutions at pH 7.0 with concentrations ranging from 20 to 60 $\mu\text{g/ml}$ were prepared. The absorbance of these solutions was measured at 296 nm, resulting in a linear plot of the absorbance versus concentration. The regression equation obtained from the plot was $y = 0.0113x - 6.68 \times 10^{-4}$, and the correlation coefficient (R^2) was 1.000.

For Cur, a calibration plot was constructed using ethanol 96% as the solvent, at concentrations ranging from 2 to 10 $\mu\text{g/ml}$. The absorbance was measured at 426 nm. The resulting calibration plot exhibited a linear relationship between absorbance and concentration. The regression equation derived from the plot was $y = 0.0633x + 7.5 \times 10^{-4}$, and the coefficient of determination (R^2) was determined to be 0.999.

Release kinetics

A dialysis-based assay was performed to measure Cur and SCA release. The solid formulation containing Cur and SCA was dispersed in 1.0 ml of artificial colonic fluid (ACF) and transferred to a prehydrated dialysis bag (MWCO:14 kDa). The dialysis bag was then immersed in 10 ml of ACF, to which 1% w/v polysorbate was added to serve as the release medium. The system was maintained at 37°C and stirred magnetically at 100 rpm.

Aliquots of 2.0 ml were withdrawn at specific intervals ranging from 15 minutes to 24 hours. The total volume was maintained at a constant level by adding a fresh medium. The amounts of released Cur and SCA were measured using UV spectrophotometry at wavelengths of 426 and 296 nm, respectively.

The cumulative release (Q) was calculated using Equation 3, which involves the volume of the release medium (V) and concentration of Cur or SCA at a given time (C_n and C_i , respectively). The volume of the former aliquots was represented by V_i .

$$Q = C_n V + \sum_{i=1}^{n-1} C_i V_i \quad (3)$$

The ACF was prepared using phosphate buffer (pH 7.4). To prepare this, 8 g of sodium chloride, 0.2 g of potassium chloride, 1.44 g of disodium phosphate, and monosodium phosphate (0.245 g) were mixed with 800 ml of distilled water. The pH was adjusted to 7.4 and diluted to 1,000 ml.

Mucoadhesion assay

An *in vitro* mucoadhesion assay was performed using murine colonic membranes. After sacrifice, colon tissue was excised immediately, thoroughly rinsed with ACF, and

inverted to expose the mucosal surface. The colonic membrane, previously filled with 2 ml of ACF, was sealed and immersed in 10 ml of the dispersion of the formulation in ACF and stirred at a constant rate of 350 rpm at 37°C for 30 minutes. The concentration of nanoparticles in the aqueous dispersions was indirectly determined by measuring their transmittance at 540 nm using a Shimadzu UV-1800 spectrophotometer.

RESULTS AND DISCUSSIONS

In this study, copolymers of mPEG-b-PCL were used as precursors for nanostructured vehicles of Cur and SCA. The copolymers were synthesized via ring-opening polymerization (ROP), starting from mPEG with a molecular weight (M_n) of 2 kDa to obtain PCL segments of 30 and 40 kDa (Fig. 1a). They were characterized by ^1H NMR to determine their molecular weights and reaction yields using mPEG as a reference, and to confirm that the polymerization reaction took place (Fig. 1b). Likewise, the molecular weight dispersion indices ($\text{Đ} = M_w/M_n$) were measured using gel permeation chromatography (GPC). The main characteristics of the synthesized copolymers are listed in Table 1.

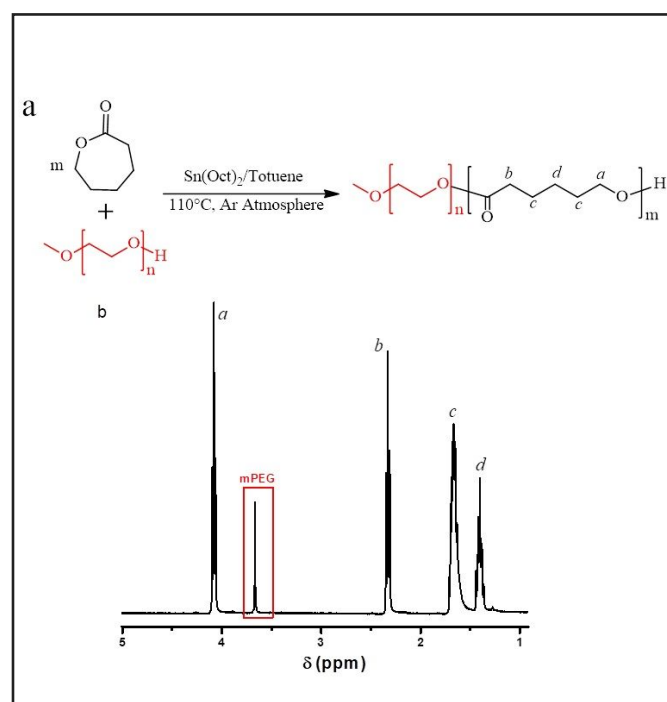


Figure 1. (a) The synthetic route used to obtain the copolymer PEG-b-PCL via ROP and (b) a representative ^1H NMR spectra of a copolymer with a molecular weight of PCL segment of 40 kDa.

Table 1. Characterization of ABCs by ^1H NMR and GPC.

Sample	^1H NMR results		Đ by GPC
	Yield (%)	M_n of PCL block (kDa)	
PEG-b-PCL 30 kDa	89	29.7	1.34
PEG-b-PCL 40 kDa	92	40.3	1.42

mPEG-b-PCL is an amphiphilic block copolymer (ABC) that self-assembles to generate core-shell nanoparticles, where the mPEG segment is oriented to a hydrophilic environment. ABCs tend to form micelle-like arrangements; however, when PCL possesses a high molecular weight, the resulting particles have poor solubility in water, which in turn reduces processes such as unimer exchange that characterize micellar structures, resulting in polymer aggregates with higher stability against dilution.

Encapsulation of Cur and SCA in the polymer nanoparticles was achieved using a double-emulsion procedure (Fig. 2). An initial emulsion (w_1/o), composed of an aqueous solution of SCA, was dispersed in an organic phase containing PEG-b-PCL and Cur dissolved in DCM. The resulting emulsion was dispersed in water in the presence of a stabilizer (PVA or CH) to obtain a double emulsion ($(w_1/o)/w_2$). Polymer nanocapsules were produced after evaporation of DCM and recovered by freeze-drying. Initially, parameters such as the type of stabilizer, drug concentration, and the molecular weight of the PCL segment of the copolymer were evaluated.

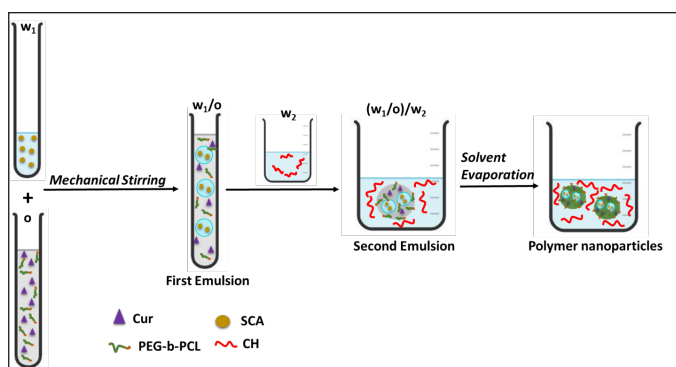


Figure 2. Schematic representation of the double emulsion process used to obtain simultaneous encapsulation of Cur and SCA.

Effect of stabilizer

Entries 1 to 3 in Table 2 show the systems stabilized using PVA 0.5% and CH at concentrations of 0.2%, 0.5%, and 0.5%. PVA, a commonly used nonionic water-soluble polymer that acts as a protective colloid for emulsion stabilization, resulted in the smallest particle size (203 nm) with a narrow distribution. However, the use of more concentrated CH as a stabilizer resulted in higher drug encapsulation. Specifically, CH at 0.5% by weight not only stabilized the emulsion drops, producing 355 nm particles under the same conditions but also increased the %EE of both drugs compared to when PVA was used as a stabilizer.

CH possesses amine groups that impart basic characteristics to the polymer and exhibits a pKa value of 6.5 [27]. Therefore, CH protonation increases at a low pH, which improves its solubility in water, resulting in chain disentanglement that affects the rheological properties of the system, providing a stabilizing effect. The increased %EE of Cur and SCA could be due to non-polar forces such as van der Waals forces, hydrogen bonds, and electrostatic interactions between the drugs and CH, as previously reported for nanoparticles composed of acetylsalicylic acid and CH [28].

Amount of Cur and SCA in the feed

In Table 2, entries 4-6 demonstrate that, as the feed amount of Cur increased, the %EE decreased. Conversely, higher efficiencies were observed for SCA as its initial amount increased, whereas the opposite trend was observed for Cur. Cur encapsulation was achieved through solubilization in the PCL domains. As a result, Cur solubility increased until PCL saturation, and the amount of loaded Cur became nearly constant. In contrast, SCA did not interact with the PCL domains and remained in the inner compartments, causing the amount of encapsulated drug to increase with the feed amount of the drug.

Table 2. %EE, particle size, and PDI of each of the systems elaborated with different external stabilizers (CH and PVA) at different concentrations of actives and M_n of PCL.

Entry	Mn of PCL (kDa)	Initial Drug concentration (mg/ml)		External stabilizer	EE (%)		DLS characterization	
		SCA	Cur		SCA	Cur	D_h (nm)	PDI
1		8	1	PVA 0.5 %	26.00	7.08	203	0.202
2	40	8	1	CH 0.2%	64.79	0.08	721	0.692
3		8	1		90.72	13.70	355	0.233
4		4	1		65.13	0.40	-	-
5		6	2		70.59	0.22	-	-
6		8	3	CH 0.5%	85.67	0.08	-	-
7	30	0	0		0.00	0.00	415	0.270
8		0	1		0.00	0.37	490	0.370
9		8	0		80.90	0	546	0.310
10		8	1		85.67	0.40	296	0.190

PDI: Polydispersity index.

Effect of molecular weight of PCL

Two copolymers with PEG blocks of 2 kDa and PCL segments of 30 and 40 kDa were compared to encapsulate SCA and Cur, respectively (Table 1, Entries 3 and 10). The results showed that the 40 kDa PCL increased Cur encapsulation and reduced particle size compared to the 30 kDa. SCA encapsulation also increased but to a lesser extent. This trend suggests that Cur encapsulation is favored by slower phase separation due to the higher PCL molecular weight, whereas SCA encapsulation is less affected by PCL length.

Effect of interactions between the drugs

To examine the impact of simultaneous encapsulation on particle %EE and size, experiments 7–10 were performed (Table 2). Empty particles were 415 nm in size, but their diameter increased in the presence of SCA and Cur and was the highest when both were co-encapsulated. This may be due to the increased interfacial tension in the second emulsion caused by the interaction of the drugs with hydrophilic segments, leading to the formation of larger particles. However, the %EE of each drug was not affected by the presence of the other drugs.

DSC characterization was conducted to investigate the effects of the drugs on the copolymer morphology. The analysis was performed on freeze-dried empty nanoparticles and formulations containing Cur, SCA, or both (Table 2, entries 7–10). The samples were cooled from room temperature to -20°C and heated to 200°C at a rate of $5^{\circ}\text{C}/\text{minute}$. The DSC traces obtained during heating (Fig. 3) show that the empty nanoparticles had a broad endothermic peak centered at 59°C , indicating the melting of the PCL crystalline domains and possibly PEG [10]. Because the molecular weight of PEG is low, it is likely miscible with PCL [29]. Upon the addition of Cur or both components to the nanoparticles, the endothermic peak associated with melting shifted to a lower temperature. The peak shifted by 53°C for Cur and a mixture of the components. This suggests that the crystalline domains in the nanoparticles were smaller and the mobility of the PCL segments was more

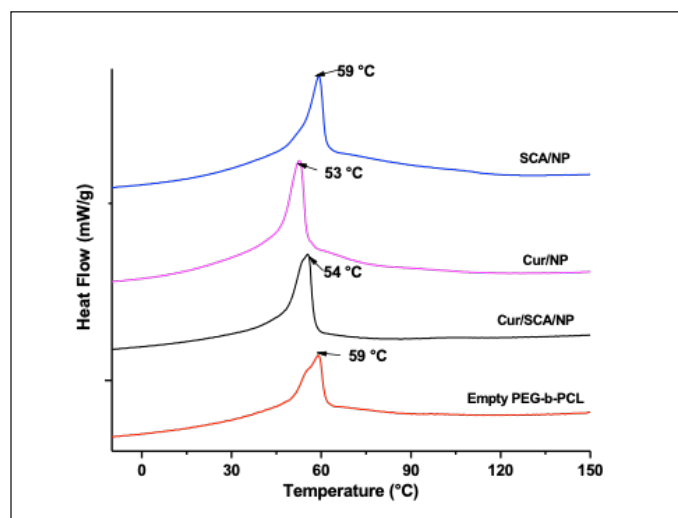


Figure 3. DSC traces of freeze-dried polymer nanoparticles formed from PEG-b-PCL with a PCL segment of 30 kDa were obtained by heating at $5^{\circ}\text{C}/\text{minute}$.

restricted. This effect was not observed in the presence of SCA, which is in agreement with the lower miscibility of PCL domains. The absence of peaks corresponding to the melting of Cur or SCA indicated that these drugs interacted with the polymer phase and did not form crystalline arrangements [30]. The simultaneous presence of both drugs did not provoke any significant effect on the thermograms, suggesting that nanoparticles presented bicompartamental characteristics.

Characterization of a selected formulation

The formulation described in entry 3 of Table 2 (designated as Cur/SCA/NP) was selected for more detailed morphological and pharmacotechnical analyses. This formulation was selected based on its smaller particle size and highest %EE.

Particle size and morphology

The morphological characteristics of the Cur/SCA/NP formulation were analyzed using SEM and compared with those of empty nanoparticles, as shown in Figure 4a and b. The images indicate that both samples are composed of spherical nanoparticles with few aggregates. The insets in Figure 4a and b demonstrate that in the presence of Cur and SCA, the diameters of most of the particles were in the range of 100–200 nm, in contrast to the unloaded particles, whose diameters ranged between 120 and 260 nm. Moreover, the empty nanoparticles exhibited a narrower diameter distribution than drug-containing particles. The hydrodynamic diameter distribution (in number) of the particles was analyzed by DLS, as shown in Figure 4c and d. The plots exhibit a similar trend to those obtained by SEM; however, the larger sizes can be attributed to particle swelling in the aqueous solution caused by the presence of hydrophilic polymer chains. In addition, the presence of certain aggregates in the SEM images suggests that they may have formed during the drying process of the dispersion droplets, resulting in the particles being pulled together. Therefore, the characterization of the Cur/SCA/NP formulation using SEM and DLS indicated that the drugs contributed to stabilizing the initial emulsions, resulting in a reduction in particle size.

Release kinetics

To characterize the release behavior of the Cur/SCA/NP system described in Table 1 (entry 3), a dialysis bag was loaded with the solid formulation dispersed in ACF and placed in a release medium composed of ACF and polysorbate 80, to ensure sink conditions. The concentrations of Cur and SCA were monitored for 24 hours and their profiles are shown in Figure 5. The initial release of both drugs exhibited a burst during the first 15 minutes, releasing 9% Cur and 18% SCA, respectively. Subsequently, the release rate increased with time, demonstrating a sustained release behavior.

The release kinetics of Cur and SCA were analyzed using the Korsmeyer-Peppas release model, and the obtained parameters are shown in the inset of Figure 5 [31]. The n values indicate that the release mechanism of both drugs deviates from Fickian diffusion, probably because of the broad distribution of particle size. The K value indicated that the release rate of SCA was higher than that of Cur, which can be attributed to the higher

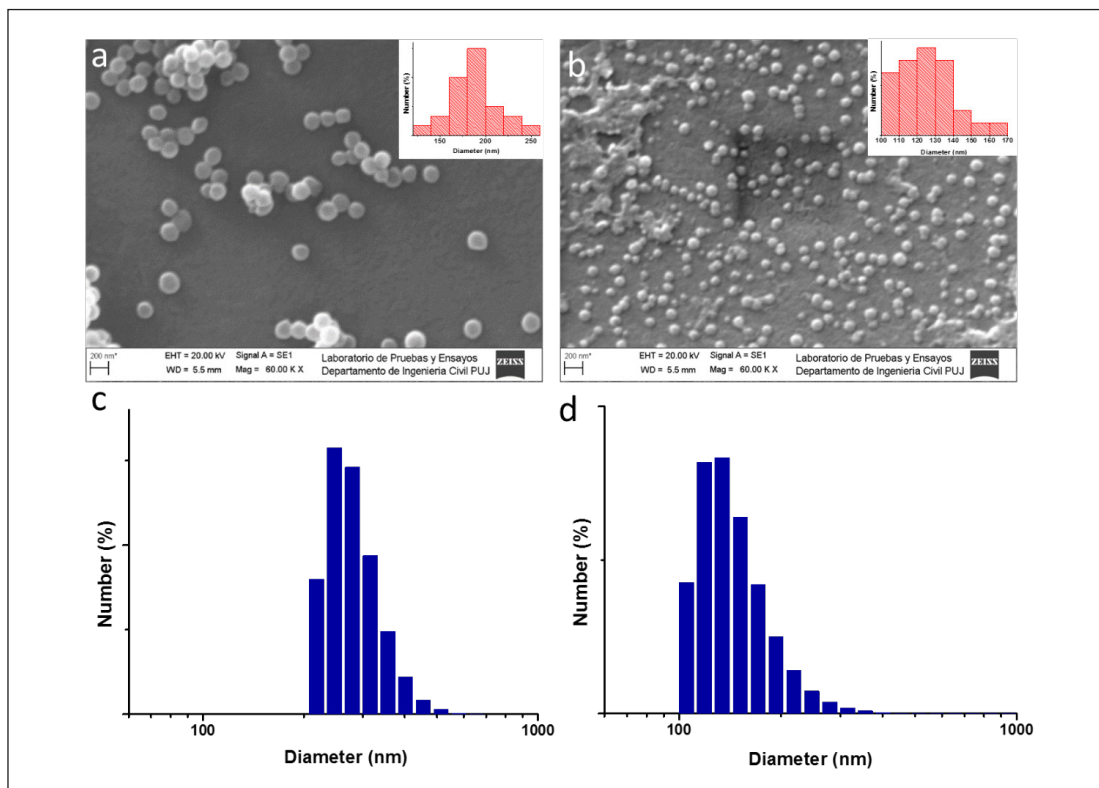


Figure 4. (a) SEM images of empty nanoparticles and (b) Cur/SCA/NP (entry 3, Table 1), and (c and d) the diameter number distributions obtained by DLS.

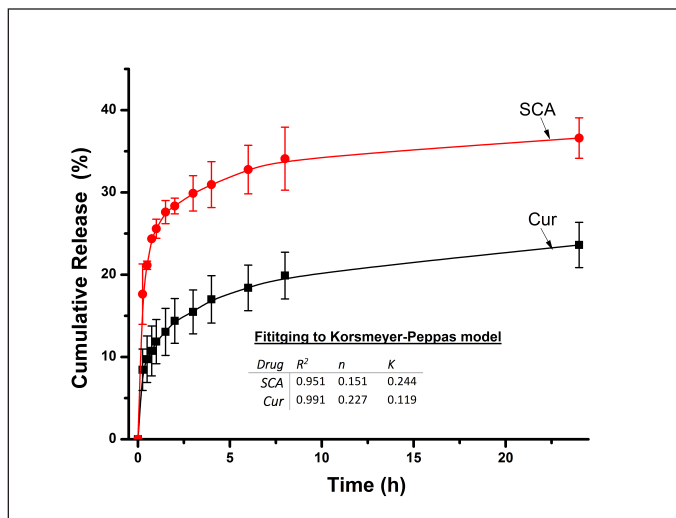


Figure 5. SCA and Cur release profiles over 24 hours from Cur/SAC/NPs (Table 1, entry 3) at 37°C in ACF with polysorbate 80 as the release medium. The profiles were fitted to Korsmeyer-Peppas, and the corresponding parameters are presented in the inset.

solubility of SCA in the release medium. This is because, at the pH of ACF, this substance is highly ionized ($pK_{a1} = 2.97$) [32]. However, the release of Cur was limited by its solubility in ACF and influenced by the presence of the surfactant polysorbate 80.

In vitro assays provide valuable insights into the release of drugs under controlled conditions in homogeneous media.

Table 3. Mucoadhesion assay results.

% T_b	% T_c	% T_i	% T_s
100	79,05	63,85	72.44
% Initial solids ($T_b - T_i$)	% Solids released by the colonic membrane ($T_b - T_c$)	% solids after treatment ($T_b - T_s - T_i$)	% Mucoadhesion $\left(\frac{T_s - T_c}{T_b - T_i} \times 100 \right)$
36.15	20.95	6.62	81.70

T_b : Transmittance of the ACF blank, T_c : Transmittance of the control (ACF exposed to the colonic membrane), T_i : transmittance of initial dispersion, T_s : transmittance of the dispersion after being exposed to the colonic membrane.

However, it is important to consider that *in vivo* conditions involve the interaction of the polymers forming nanoparticles with physiological constituents and lipophilic molecules that could particularly complex Cur. These interactions have the potential to enhance the drug release rate [33,34].

Mucoadhesion assay

The mucoadhesion percentage of the formulation described in Table 1 (entry 3) was analyzed, and the results are presented in Table 3. After 30 minutes of contact with the colonic membrane, nanoparticles showed a mucoadhesion rate of 81.7%. This high value indicated that a significant number of nanoparticles remained adsorbed on the intestinal tissue. The positive surface charge of the nanoparticles imparted by

CH, a component of the system, is responsible for this high mucoadhesion rate. Even at pH values close to neutral, the amino groups on CH were partially protonated, resulting in a positive surface charge, as demonstrated by the zeta potential value of $+71.1 \pm 1.3$. In contrast, the predominantly negative surface charge of colonic cells is due to the presence of negative sialic acid residues in the intestinal mucins. The opposite charge of nanoparticles and colonic cells results in strong electrostatic interactions, allowing for effective adhesion and the observed phenomenon of mucoadhesion, as previously described [35].

CONCLUSION

In this study, we co-encapsulated Cur and SCA, two naturally occurring derivatives known for their anticancer properties against colon cancer, in mucoadhesive nanoparticles. A double emulsification process was employed using the PEG-b-PCL copolymer as the precursor, resulting in spherical nanoparticles with sizes <500 nm. To confer mucoadhesive properties, CH was used as a stabilizer for the second emulsion, owing to its protonable amine groups. The PEG-b-PCL copolymer, with a molecular weight of 40 kDa, exhibited the highest EE for both Cur and SCA. The polymer nanoparticles loaded with both drugs demonstrated sustained release for up to 24 hours. These findings demonstrate the utility of the double emulsion method for co-encapsulating drugs with diverse chemical characteristics, thus enabling their potential for combined therapies.

ACKNOWLEDGMENT

The authors acknowledge the financial support provided by Minciencias Colombia through grant number 187-2019.

AUTHOR CONTRIBUTIONS

All authors made substantial contributions to the conception and design, acquisition of data, or analysis and interpretation of data; took part in drafting the article or revising it critically for important intellectual content; agreed to submit to the current journal; gave final approval of the version to be published; and agree to be accountable for all aspects of the work. All the authors are eligible to be an author as per the international committee of medical journal editors (ICMJE) requirements/guidelines.

CONFLICTS OF INTEREST

The authors report no financial or any other conflicts of interest in this work.

ETHICAL APPROVALS

This study was approved by the ethics committee of the same institution through Act Number 15 of 7 April 2022 of the Faculty Council, Resolution 28 of 2022.

DATA AVAILABILITY

All data generated and analyzed are included in this research article.

PUBLISHER'S NOTE

This journal remains neutral with regard to jurisdictional claims in published institutional affiliation.

REFERENCES

- Sung H, Ferlay J, Siegel RL, Laversanne M, Soerjomataram I, Jemal A, *et al.* Global cancer statistics 2020: Globocan estimates of incidence and mortality worldwide for 36 cancers in 185 countries. *CA Cancer J Clin.* 2021;71:209–49.
- Piñeros M, Laversanne M, Barrios E, de Camargo Cancela M, de Vries E, Pardo C, *et al.* An updated profile of the cancer burden, patterns and trends in Latin America and the Caribbean. *Lancet Reg Health Am.* 2022;13:100294.
- Mohammadi H, Shokrzadeh M, Akbari-Dafsari O, Amani N, Modanlou M, Mohammadpour A, *et al.* Evaluation of curcumin nano-micelle on proliferation and apoptosis of ht29 and hct116 colon cancer cell lines. *Middle East J Cancer.* 2022;13:99–109.
- Johnson JJ, Mukhtar H. Curcumin for chemoprevention of colon cancer. *Cancer Lett.* 2007;255:170–81.
- Selvam C, Prabu SL, Jordan BC, Purushothaman Y, Umamaheswari A, Zare MSH, *et al.* Molecular mechanisms of curcumin and its analogs in colon cancer prevention and treatment. *Life Sci.* 2019;239:117032.
- Salah N, Dubuquoy L, Carpentier R, Betbeder D. Starch nanoparticles improve curcumin-induced production of anti-inflammatory cytokines in intestinal epithelial cells. *Int J Pharm X.* 2022;4:100114.
- Kunnumakkara AB, Harsha C, Banik K, Vikkurthi R, Sailo BL, Bordoloi D, *et al.* Is curcumin bioavailability a problem in humans: lessons from clinical trials. *Expert Opin Drug Metab Toxicol.* 2019;15:705–33.
- Drew JE, Arthur JR, Farquharson AJ, Russell WR, Morrice PC, Duthie GG. Salicylic acid modulates oxidative stress and glutathione peroxidase activity in the rat colon. *Biochem Pharmacol.* 2005;70:888–93.
- Zitta K, Meybohm P, Bein B, Huang Y, Heinrich C, Scholz J, *et al.* Salicylic acid induces apoptosis in colon carcinoma cells grown *in-vitro*: influence of oxygen and salicylic acid concentration. *Exp Cell Res.* 2012;318:828–34.
- Angarita AV, Umaña-Perez A, Perez LD. Enhancing the performance of peg-b-pcl-based nanocarriers for curcumin through its conjugation with lipophilic biomolecules. *J Bioact Compat Polym.* 2020;35:399–413.
- Bansal SS, Goel M, Aqil F, Vadhanam MV, Gupta RC. Advanced drug delivery systems of curcumin for cancer chemoprevention. *Cancer Prev Res.* 2011;4:1158–71.
- Feng T, Wei Y, Lee RJ, Zhao L. Liposomal curcumin and its application in cancer. *Int J Nanomed.* 2017;12:6027.
- Cheng C, Wu Z, McClements DJ, Zou L, Peng S, Zhou W, *et al.* Improvement on stability, loading capacity and sustained release of rhamnolipids modified curcumin liposomes. *Colloids Surf B Biointerfaces.* 2019;183:110460.
- Sampedro-Guerrero J, Vives-Peris V, Gomez-Cadenas A, Clausell-Terol C. Improvement of salicylic acid biological effect through its encapsulation with silica or chitosan. *Int J Biol Macromol.* 2022;199:108–20.
- Kurczewska J, Ratajczak M, Gajecka M. Alginate and pectin films covering halloysite with encapsulated salicylic acid as food packaging components. *Appl Clay Sci.* 2021;214:106270.
- Bhalerao S, Raje Harshal A. Preparation, optimization, characterization, and stability studies of salicylic acid liposomes. *Drug Dev Ind Pharm.* 2003;29:451–67.
- Woodruff MA, Hutmacher DW. The return of a forgotten polymer—polycaprolactone in the 21st century. *Prog Polym Sci.* 2010;35:1217–56.
- Zou T, Dembele F, Beugnet A, Sengmanivong L, Trepout S, Marco S, *et al.* Nanobody-functionalized peg-b-pcl polymersomes and their targeting study. *J Biotechnol.* 2015;214:147–55.
- Ways TMM, Lau WM, Khutoryanskiy VV. Chitosan and its derivatives for application in mucoadhesive drug delivery systems. *Polymers.* 2018;10:267.

20. Fernandes M, Gonçalves IC, Nardecchia S, Amaral IF, Barbosa MA, Martins MCL. Modulation of stability and mucoadhesive properties of chitosan microspheres for therapeutic gastric application. *Int J Pharm.* 2013;454:116–24.
21. Hua S, Marks E, Schneider JJ, Keely S. Advances in oral nano-delivery systems for colon targeted drug delivery in inflammatory bowel disease: selective targeting to diseased versus healthy tissue. *Nanomed Nanotechnol Biol Med.* 2015;11:1117–32.
22. Belali N, Wathoni N, Muchtaridi M. Advances in orally targeted drug delivery to colon. *J Adv Pharm Technol Res.* 2019;10:100.
23. Tozaki H, Odoriba T, Okada N, Fujita T, Terabe A, Suzuki T, *et al.* Chitosan capsules for colon-specific drug delivery: enhanced localization of 5-aminosalicylic acid in the large intestine accelerates healing of tnbs-induced colitis in rats. *J Control Release.* 2002;82:51–61. [https://doi.org/https://doi.org/10.1016/S0168-3659\(02\)00084-6](https://doi.org/https://doi.org/10.1016/S0168-3659(02)00084-6)
24. Arias ER, Angarita-Villamizar V, Baena Y, Parra-Giraldo C, Perez LD. Phospholipid-conjugated peg-b-pcl copolymers as precursors of micellar vehicles for amphotericin B. *Polymers.* 2021;13:1747.
25. Rodriguez YJ, Quejada LF, Villamil JC, Baena Y, Parra-Giraldo CM, Perez LD. Development of amphotericin B micellar formulations based on copolymers of poly (ethylene glycol) and poly (ϵ -caprolactone) conjugated with retinol. *Pharmaceutics.* 2020;12:196.
26. Umerska A, Gaucher C, Oyarzun-Ampuero F, Fries-Raeth I, Colin F, Villamizar-Sarmiento MG, *et al.* Polymeric nanoparticles for increasing oral bioavailability of curcumin. *Antioxidants.* 2018;7:46.
27. Domard A. Ph and cd measurements on a fully deacetylated chitosan: application to cuii—polymer interactions. *Int J Biol Macromol.* 1987;9:98–104.
28. Luo S, Man H, Jia X, Li Y, Pan A, Zhang X, *et al.* Preparation and characterization of acetylsalicylic acid/chitosan nanoparticles and its antithrombotic effects. *Des Monomers Polym.* 2018;21:172–81.
29. Liu F, Goldenfeld N. Dynamics of phase separation in block copolymer melts. *Phys Rev A.* 1989;39:4805.
30. Carrascal JJ, Pinal R, Carvajal T, Pérez LD, Baena Y. Benzoic acid complexes with eudragit e100®: new alternative antimicrobial preservatives. *Int J Pharm.* 2021;607:120991. <https://doi.org/https://doi.org/10.1016/j.ijpharm.2021.120991>
31. Wu IY, Bala S, Škalko-Basnet N, Di Cagno MP. Interpreting non-linear drug diffusion data: utilizing korsmeyer-peppas model to study drug release from liposomes. *Eur J Pharm Sci.* 2019;138:105026.
32. Hasanain F, Wang ZY. New one-step synthesis of polyimides in salicylic acid. *Polymer.* 2008;49:831–5.
33. Wang Y, Wang J, Zhu D, Wang Y, Qing G, Zhang Y, *et al.* Effect of physicochemical properties on *in vivo* fate of nanoparticle-based cancer immunotherapies. *Acta Pharm Sin B.* 2021;11:886–902.
34. Cai Y, Qi J, Lu Y, He H, Wu W. The *in vivo* fate of polymeric micelles. *Adv Drug Deliv Rev.* 2022;188:114463.
35. Chuah LH, Billa N, Roberts CJ, Burley JC, Manickam S. Curcumin-containing chitosan nanoparticles as a potential mucoadhesive delivery system to the colon. *Pharm Dev Technol.* 2013;18:591–9.

How to cite this article:

Moreno C, Forero J, Baena Y, Perez L. Co-encapsulation of curcumin and salicylic acid in mucoadhesive polymer nanoparticles. *J Appl Pharm Sci.* 2024;14(01):189–196.